ORGANOMETALLICS

Article

pubs.acs.org/Organometallics

Role of Zr,Al Hydride Intermediate Structure and Dynamics in Alkene Hydroalumination with XAlBu$^i_2$ (X = H, Cl, Bu^i), Catalyzed by Zr η^5 Complexes

Lyudmila V. Parfenova,*[†] Pavel V. Kovyazin,[†] Ilya E. Nifant'ev,[‡] Leonard M. Khalilov,[†]
and Usein M. Dzhemilev[†]

[†]Institute of Petrochemistry and Catalysis, Russian Academy of Sciences, prospect Oktyabrya, 141, 450075 Ufa, Russian Federation
[‡]Department of Chemistry, Lomonosov Moscow State University, 1-3 Leninskiye Gory, 119991 Moscow, Russian Federation

Supporting Information

ABSTRACT: The zirconocene complexes L_2ZrCl_2 (L = C_5H_5, C_5H_4Me, Ind, C_5Me_5; L_2 = *rac*-$Me_2C(2\text{-}Me\text{-}4\text{-}Bu^t\text{-}C_5H_2)_2$, *meso*-$Me_2C(2\text{-}Me\text{-}4\text{-}Bu^t\text{-}C_5H_2)_2$, *rac*-$Me_2C(3\text{-}Bu^t\text{-}C_5H_3)_2$, *rac*-$Me_2C(Ind)_2$, *rac*-$Me_2Si(Ind)_2$, and *rac*-$C_2H_4(Ind)_2$) were tested as catalysts in alkene hydroalumination by the isobutylalanes $XAlBu^i_2$ (X = H, Cl, Bu^i). A low-temperature NMR spectroscopy study on the structure and dynamics of Zr,Al intermediates formed in the L_2ZrCl_2−$XAlBu^i_2$ systems showed that the intra- and intermolecular exchange in the bimetallic clusters, controlled by the steric factor of the η^5 ligand and organoaluminum compound nature, determines the activity of the whole catalytic system.

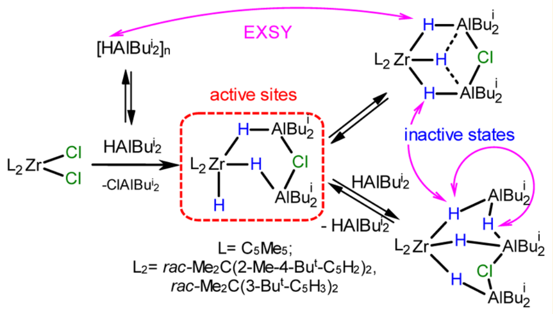

INTRODUCTION

Catalytic alkene hydroalumination has found wide use in organic and organometallic synthesis as an efficient method for the synthesis of practically important organoaluminum compounds (OACs) of a specified structure and as a method for regioselective reduction and functionalization of unsaturated compounds.[1] This type of reaction can be catalyzed by complexes of various transition metals (Ti, Zr, V, Cr, Mn, Fe, Co, Ni, Cu, Zn, etc.). It is noted that the activity of the catalytic system is strongly affected by both the nature of substituents in the initial OAC and the electronic structure of the transition metal.[2] Various bimetallic hydride intermediates are assumed as active centers of the reactions.[3]

The catalytic action of zirconocene complexes in alkene hydroalumination is of considerable interest, since these compounds not only perform the reaction under mild conditions with high regio- and stereoselectivity but also allow establishment of the reaction mechanism, particularly, the intermediate structure and interconversions using dynamic NMR spectroscopy, which provides the most complete information and allows direct monitoring of the reaction. Extensive application of this method to the studies of catalytic systems based on zirconium η^5 complexes and OACs became possible due to several reasons. First, a broad range of catalytic reactions can be implemented in these systems, from hydro-, carbo-, and cyclometalation to polymerization of unsaturated compounds. Second, these systems are convenient for fundamental investigations, since η^5 ligands bound to zirconium atoms act like magnetic probes reflecting the electronic state of the transition-metal atom. Furthermore, the reaction times appear to be convenient for monitoring, as well as the absence of paramagnetic species, which, for example, in the case of titanium complexes preclude observation of the genesis of intermediate complexes of catalytic systems due to pronounced NMR signal broadening.

Experimental studies of the mechanism of alkene hydroalumination with $XAlBu^i_2$ (where X = H, Cl, Bu^i) in the presence of Cp_2ZrCl_2 by dynamic NMR demonstrated that bimetallic Al,Zr-hydride complexes may act as the key reaction intermediates.[4,5] A quantum chemical study of this reaction[6] specified the initial steps of the ligand exchange between $HAlBu^i_2$ and Cp_2ZrCl_2 and proposed the structure of bimetallic intermediates that can exist in the system (Scheme 1). Among the intermediates, complexes **6a**, **7a**, and **11a** were found experimentally.[4,5,7] The possibility of complex **10a** formation has been considered in the literature[8] as well. Further theoretical studies demonstrated[9] that intermediates **3a**, **4a**, and **5a** containing a free Zr−H bond can act as catalytically active sites of the hydroalumination, and the reactivity of these complexes is dependent on the number of bridging Zr−H−Al bonds: the greater their number, the less active the complex becomes.

An introduction of activating agents (MAO or $[Ph_3C][B(C_6F_5)_4]$) into the catalytic systems L_2ZrCl_2−$XAlBu^i_2$ makes possible the polymerization of the unsaturated compounds.[10] It is assumed that neutral or cationic bimetallic hydride complexes containing $[L_2ZrH_3]$ or $[L_2ZrH_2]$ moieties, depending on the

Received: April 30, 2015

DOI: 10.1021/acs.organomet.5b00370

Scheme 1. Quantum Chemical Model of Catalytic Alkene Hydroalumination by $HAlBu^i_2$

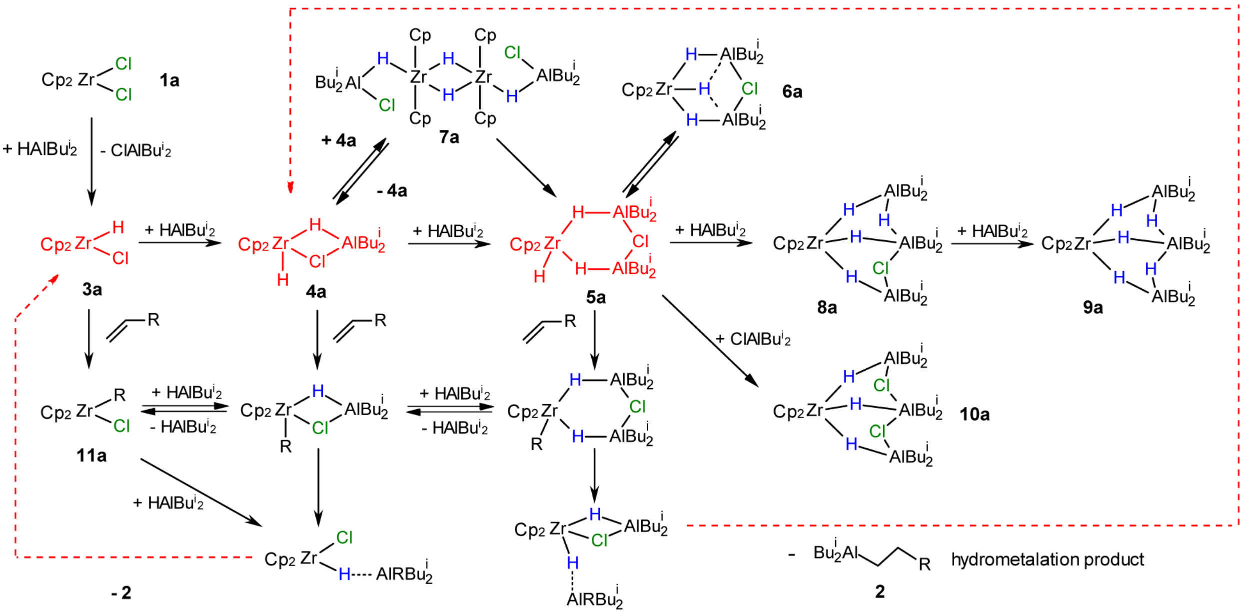

nature of the η^5 ligand, are formed as intermediates in the reaction.[8,11,12]

However, the question of how the OAC and zirconocene structures affect the activity of these catalytic systems remains open. To solve the problem, we studied the structure, dynamics, and reactivity of the bimetallic hydride complexes formed in the reaction of L_2ZrCl_2 with $XAlBu^i_2$ and considered these results in the context of the catalytic system efficiency in the alkene hydroaluminations.

RESULTS AND DISCUSSION

Catalytic Activity of Zr η^5 Complexes in the Hydroalumination of Terminal Alkenes with $XAlBu^i_2$ (X = H, Cl, Bu^i). In order to elucidate the factors determining the activity of the hydroaluminating catalytic systems, we studied the catalytic action of zirconocene complexes L_2ZrCl_2 (**1a**–**j**: L = C_5H_5 (**a**), C_5H_4Me (**b**), C_5Me_5 (**c**); L_2 = *rac*-$Me_2C(2\text{-}Me\text{-}4\text{-}Bu^t\text{-}C_5H_2)_2$ (**d**), *meso*-$Me_2C(2\text{-}Me\text{-}4\text{-}Bu^t\text{-}C_5H_2)_2$ (**e**), *rac*-$Me_2C(3\text{-}Bu^t\text{-}C_5H_3)_2$ (**f**), Ind (**g**); *rac*-$Me_2C(Ind)_2$ (**h**), *rac*-$Me_2Si(Ind)_2$ (**i**), *rac*-$C_2H_4(Ind)_2$ (**j**)) in alkene hydroalumination with the isobutylalanes $XAlBu^i_2$ (X = H, Cl, Bu^i) (Scheme 2). The reaction yields the hydroalumination products **2**.

Previously, we demonstrated[4] that, in the presence of complex **1a**, at a reactant molar ratio **1a**:OAC:alkene of 1:60:50, the highest hydroalumination rate among the chosen OACs was observed for $AlBu^i_3$. In the case of $ClAlBu^i_2$, a long-term induction period (up to 3 h) was found.[13] Diisobutylaluminum hydride showed the lowest activity among the studied OACs (Figure 1a).

The catalysis by complex **1b** leads almost to the same results; however, in the case of $ClAlBu^i_2$, the induction period disappears and the yield of hydroalumination products decreases (Figure 1b). In the presence of the most sterically hindered catalyst **1c**, the rate of alkene hydroalumination substantially increases when $HAlBu^i_2$ is used, whereas the reaction with $ClAlBu^i_2$ or $AlBu^i_3$ is slowed down (Figure 1c). A replacement of the cyclopentadienyl ligands in the zirconium complex with indenyl ligands provides a considerable decrease in the yield of the hydroalumination products irrespective of the OAC structure (Figure 1d).

Scheme 2

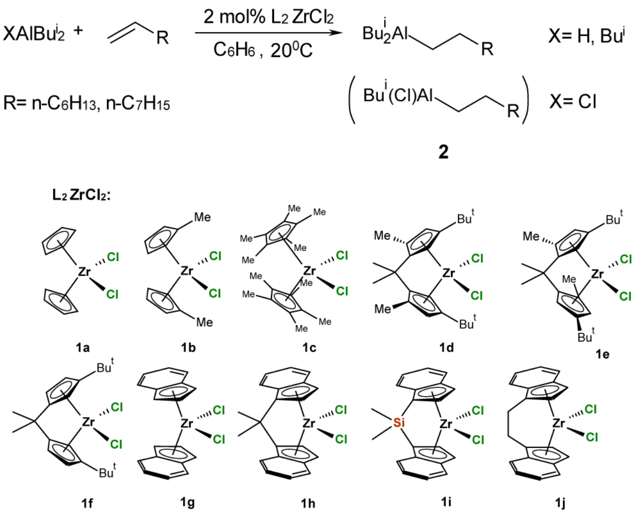

The use of *rac* isomers of complexes **1d**,**f** with bulky ligands as catalysts in the reaction of alkene with $HAlBu^i_2$ provides a high yield of hydrometalation product as well as in the case of **1c** (Figure 2). The replacement of $HAlBu^i_2$ with $AlBu^i_3$ in these systems dramatically decreases the alkene conversion. *rac*-Zirconocenes with *ansa*-indenyl ligands **1h**–**j** and the *meso* isomer of the sterically hindered bis-cyclopentadienyl complex **1e** (the starting sample of **1e** contained ~17% of **1d** impurity) showed a catalytic activity lower than that of complex **1a** in the hydroalumination with $HAlBu^i_2$.

As follows from Figure 3, conducting the reaction of alkene with $HAlBu^i_2$ in the presence of a stoichiometric amount of **1a** (**1a**:$HAlBu^i_2$:alkene ratio of 1:3:1) was accompanied by a sharp increase in the reaction rate, so that 90% conversion of the alkene was achieved in 2 h. In the catalytic version, when the initial OAC concentration was increased or the amount of the catalyst was reduced to the molar ratio **1a**:$HAlBu^i_2$:alkene 1:6:5

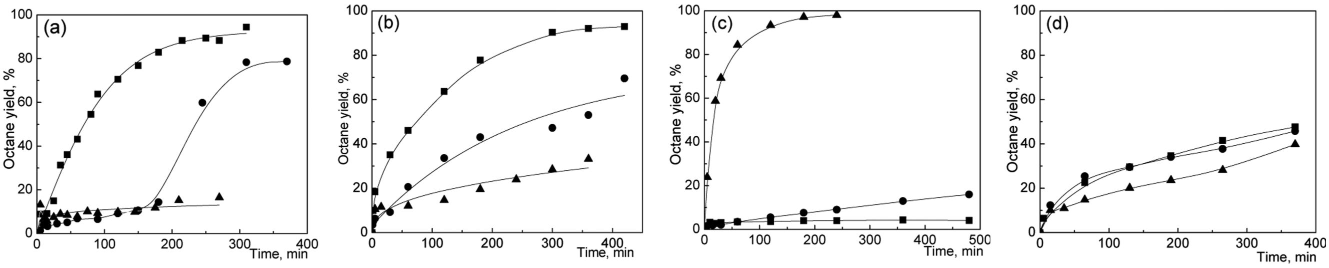

Figure 1. Effect of η^5 ligand and OAC structure ($HAlBu^i_2$ (▲), $ClAlBu^i_2$ (●), $AlBu^i_3$ (■)) on octane yield in the reaction of 1-octene hydroalumination (molar ratio L_2ZrCl_2:AOC:alkene 1:60:50, C_6H_6, t = 20 °C): (a) $(C_5H_5)_2ZrCl_2$ (**1a**); (b) $(C_5H_4Me)_2ZrCl_2$ (**1b**); (c) $(C_5Me_5)_2ZrCl_2$ (**1c**); (d) Ind_2ZrCl_2 (**1g**).

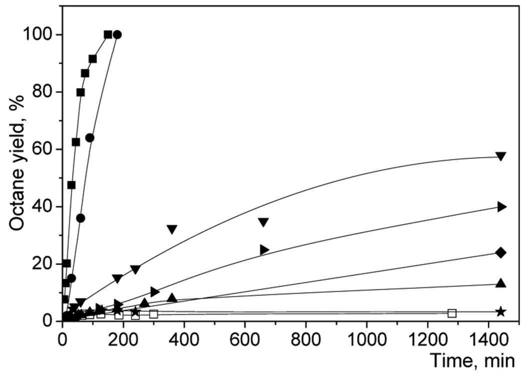

Figure 2. Activity of *ansa*-zirconocenes in the reaction of 1-octene hydroalumination by $XAlBu^i_2$ (molar ratio L_2ZrCl_2:AOC:alkene 1:60:50, C_6H_6, t = 20 °C): *rac*-$Me_2C(2\text{-}Me\text{-}4\text{-}Bu^t\text{-}C_5H_2)_2ZrCl_2$ + $HAlBu^i_2$ (■), *rac*-$Me_2C(3\text{-}Bu^t\text{-}C_5H_3)_2ZrCl_2$ + $HAlBu^i_2$ (●), *rac*-$C_2H_4(Ind)_2ZrCl_2$ + $HAlBu^i_2$ (▼), *rac*-$Me_2C(Ind)_2ZrCl_2$ + $HAlBu^i_2$ (▶), *rac*-$Me_2Si(Ind)_2ZrCl_2$ + $HAlBu^i_2$ (♦), *rac*-$Me_2C(2\text{-}Me\text{-}4\text{-}Bu^t\text{-}C_5H_2)_2ZrCl_2$ + $AlBu^i_3$ (□), *rac*-$C_2H_4(Ind)_2ZrCl_2$ + $AlBu^i_3$ (*), *meso*-$Me_2C(2\text{-}Me\text{-}4\text{-}Bu^t\text{-}C_5H_2)_2ZrCl_2$ + $HAlBu^i_2$ (▲).

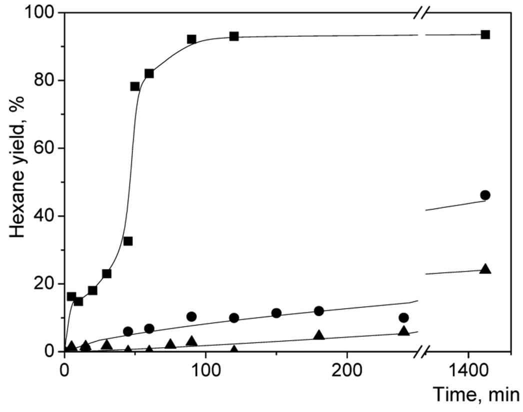

Figure 3. Hexane yield in the reaction of 1-hexene with $HAlBu^i_2$ vs amount of catalyst **1a** (C_6H_6, t = 24 °C). Molar ratio **1a**:$HAlBu^i_2$:alkene: 1:3:1 (■), 1:6:5 (●), 1:60:50 (▲).

or 1:60:50, a considerable decrease in the hydroalumination product yield was observed.

Since the rate of the catalytic hydroalumination is largely determined by the structure of the OAC, we carried out a study of solutions of $HAlBu^i_2$ and $ClAlBu^i_2$ in hydrocarbon solvents.

Exchange Spectroscopy Studies on the Structure and Dynamics of the Initial Isobutyl-Substituted OACs. The isobutyl-substituted OACs tend to self-associate to various extents. For example, it is known that in nonpolar solvents $HAlBu^i_2$ exists mainly as a trimer and $ClAlBu^i_2$ is a dimer, while $AlBu^i_3$ is monomeric.[14] Quantum chemical modeling of self-association of $HAlBu^i_2$ and $ClAlBu^i_2$ shows that, in nonpolar solvents at room temperature, the dimeric form predominates for $ClAlBu^i_2$ and a mixture of dimeric and trimeric forms prevails for $HAlBu^i_2$.[15] Although these compounds had been thoroughly studied, our experimental results made a certain contribution to the knowledge of the structure of the initial OACs. The ^1H NMR spectra of $HAlBu^i_2$ recorded at room temperature in benzene were found to exhibit signals for four hydride atoms at δ_H 3.94, 3.24, 2.97, and 2.77 ppm (Figure S1a in the Supporting Information). These signals were correlated in the EXSY spectra (no cross-peaks between them were present in the COSY spectra) (Figure 4a). A similar observation was reported previously.[12] The signal at δ_H 3.94 ppm, which was assigned to the hydride atom of the $HAlBu^i_2$ monomer, had the lowest intensity. Dimerization should be accompanied by an upfield shift of the hydride resonance line due to the formation of bridging Al−H−Al bonds. Therefore, the next signal at δ_H 3.24 ppm was assigned to the dimeric form. The most intense resonance line at δ_H 2.97 ppm corresponds to the trimer, while the highest-field signal out of the four signals (δ_H 2.77 ppm) apparently belongs to the tetramer.

When the $HAlBu^i_2$ concentration in benzene is 3.3 mol/L (in relation to the monomer), the monomer:dimer:trimer:tetramer molar ratio is 1:29:226:23 and the monomer concentration is ~4 × 10^{-3} mol/L. The addition of 0.6 equiv of $ClAlBu^i_2$ to 1 equiv of $HAlBu^i_2$ in toluene changes the $[HAlBu^i_2]$:$[(HAlBu^i_2)_2]$:$[(HAlBu^i_2)_3]$:$[(HAlBu^i_2)_4]$ molar ratio to 1:6:5:0.4 (Figure S1b in the Supporting Information). As follows from the ratio, the percentage of the diisobutylaluminum hydride monomer (δ_H 3.94 ppm) increases with the appearance of $ClAlBu^i_2$. Probably, $ClAlBu^i_2$ has an influence on the equilibrium shown in Scheme 3 by producing the mixed oligomers $[(HAlBu^i_2)_n\cdot(ClAlBu^i_2)_m]$,[16] which provide new signals in the ^1H NMR spectrum at δ_H equal to 3.47, 3.18, and 2.88 ppm (Figure S1b; T = 260 K, toluene). This fact is confirmed by the presence of slow intermolecular exchange between the mixed oligomers with $[HAlBu^i_2]_n$ in the EXSY spectrum at 260 K (Figure 4b). Thus, the involvement of the OAC monomer in the reaction with Zr complexes during the hydroalumination is quite probable. The percentage of the $HAlBu^i_2$ monomer in the system can probably increase, owing to the additional amount of $ClAlBu^i_2$ arising in the early steps upon Cl−H exchange in the L_2ZrCl_2 + $HAlBu^i_2$ reaction.

Zr,Al-Hydride Intermediates in the Reaction of L_2ZrCl_2 with $XAlBu^i_2$ (X = H, Cl, Bu^i). *A. Systems Based on the C_5H_5 Ligand.* In order to elucidate the structure and dynamics of the

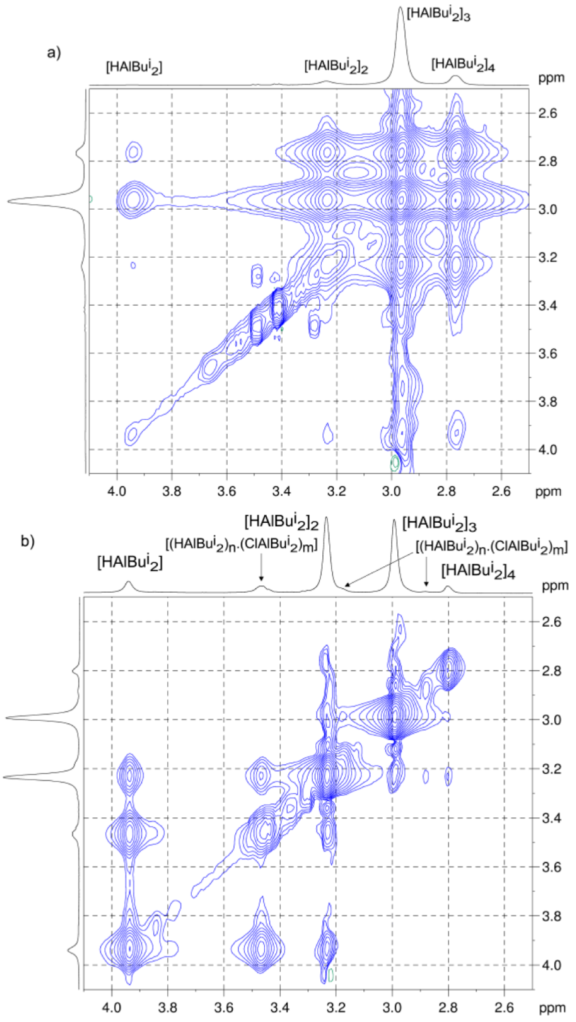

Figure 4. EXSY spectra of (a) $HAlBu^{i}_{2}$ in C_6D_6 (3.3 mol/L, 300 K, τ = 0.3 s) and (b) the mixture $HAlBu^{i}_{2}$ + $ClAlBu^{i}_{2}$ in C_7D_8 (C($HAlBu^{i}_{2}$) 1.2 mol/L, C($ClAlBu^{i}_{2}$) 0.7 mol/L, 260 K, τ = 0.3 s).

Scheme 3

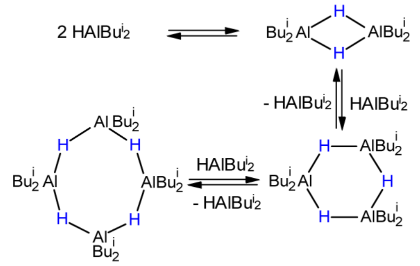

intermediates involved in catalytic hydroalumination, we studied the reaction of $(C_5H_5)_2ZrCl_2$ (**1a**) and $XAlBu^{i}_{2}$ (X = H, Bu^{i}). In the reaction with $HAlBu^{i}_{2}$, a complete dissolution of complex **1a** in d_6-benzene was observed at 20 °C and a **1a**:$HAlBu^{i}_{2}$ molar ratio of 1:3. Previously, formation of the individual compound $(C_5H_5)_2Zr(\mu\text{-}H)_3(AlBu^{i}_{2})_2(\mu\text{-}Cl)$ (**6a**)[7] or $(C_5H_5)_2Zr(\mu\text{-}H)_3(AlBu^{i}_{2})_3(\mu\text{-}Cl)_2$ (**10a**)[6,8] was assumed for this system (Scheme 1).

According to our NMR investigations, the reaction of **1a** with $HAlBu^{i}_{2}$ (1:3) yields a mixture of at least two complexes in a 2.7:1 ratio. The ^{1}H NMR spectra of this mixture recorded at 220 K (Figure 5) exhibit two signals for the Cp rings at δ_H 5.66 and 5.59 ppm and two groups of signals correlated in the COSY spectra in the region of hydride atoms bonded to Zr and Al: (a) a triplet at δ_H −1.06 ppm and a doublet at δ_H −2.30 ppm (1:2 ratio) and (b) broadened signals at δ_H 3.56, −1.22, −2.30, and −3.05 ppm (1:1:1:1 ratio) (Table 1). The more intense resonance line of the Cp ligand at δ_H 5.59 ppm was related to the triplet at δ_H −1.06 ppm in the ratio 10:1. The ratio of the areas of the cyclopentadienyl signal at δ_H 5.66 ppm and a signal at δ_H 3.56 ppm was 10:1 as well.

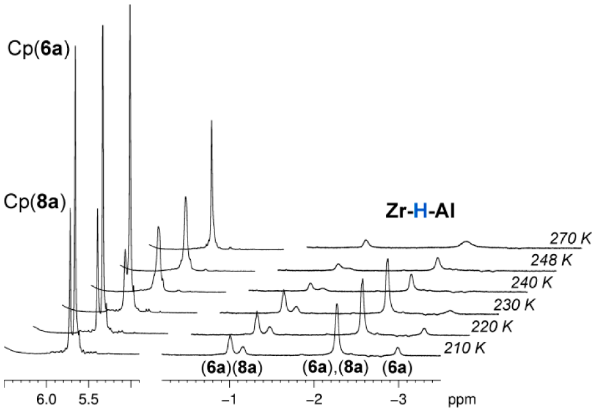

Figure 5. Variable-temperature ^{1}H NMR study on the system $(C_5H_5)_2ZrCl_2$ (**1a**)−$HAlBu^{i}_{2}$ (1:3) in C_7D_8 (the intensity of upfield signals is increased for clarity).

Thus, both complexes contain $[(C_5H_5)_2ZrH_3]$ moieties and in the latter complex the symmetry is reduced, giving rise to three nonequivalent signals in the upfield region. If one assumes that **6a** is a more symmetric complex, the symmetry may be reduced as a result of one more $HAlBu^{i}_{2}$ molecule entering, providing structure **8a**, the hydride signal of this moiety being observed in the middle part of the spectrum (Table 1). A rise in the concentration of $HAlBu^{i}_{2}$ in the mixture entails an increase in the percentage of nonsymmetric complex **8a**. In low-temperature EXSY spectra (230−240 K) slow exchange is observed between the hydride atoms of complexes **6a** and **8a** (Figure S4 in the Supporting Information). In addition, the signal at δ_H 3.56 ppm for the Al−H−Al bond of complex **8a** was correlated with the signals of oligomers of $HAlBu^{i}_{2}$. As the temperature of the reaction mixture **1a** + $HAlBu^{i}_{2}$ was increased to 300 K, gradual coalescence of signals for both the Cp ligands and hydride hydrogens took place, resulting in a single Cp resonance line at δ_H 5.69 ppm (δ_C 104.5 ppm) and broadened hydride signals at δ_H −1.00 and −2.11 ppm with a 10:1:2 ratio, respectively (Figure 5). The rate constant and the activation parameters for the dynamic process **6a** ↔ **8a** were k_{220} = 10.9 s^{-1}, $\Delta G^{\ddagger}_{220}$ = 11.98 ± 0.05 kcal/mol, $\Delta H^{\ddagger}$ = 6.11 ± 0.54 kcal/mol, and $\Delta S^{\ddagger}$ = −26.80 ± 9.97 cal/(mol K). The temperature increase provided the exchange between the hydride atoms of Zr−H−Al bonds of the complexes and the oligomers of $HAlBu^{i}_{2}$ (Figure 6). Apparently, the exchange occurs via dissociation of the Zr,Al-hydride complexes with elimination of the monomer that serves as a connecting unit between the complexes and the $[HAlBu^{i}_{2}]_n$ (Scheme 4).

We attempted to prepare complex **6a** by an alternative synthesis, namely, by the reaction of 0.5 equiv of $[(C_5H_5)_2ZrH_2]_2$ (**12a**) with 1 equiv of $ClAlBu^{i}_{2}$ and 1 equiv of $HAlBu^{i}_{2}$ (Scheme 5). The NMR chemical shifts of the bridging hydride atoms and cyclopentadienyl ligands in the

DOI: 10.1021/acs.organomet.5b00370
Organometallics XXXX, XXX, XXX−XXX

Table 1. ^{1}H NMR Spectra of Zr,Al-Hydride Complexes[a]

complex	*T*, K	Zr−H−Al	L
$(C_5H_5)_2Zr(\mu\text{-H})_3(AlBu^i_2)_2(\mu\text{-Cl})$ (**6a**)	220	−2.30 (d, 4.8 Hz, 2H) −1.06 (d, 6.8 Hz, 1H)	5.59 (s, 10H)
$(C_5H_4Me)_2Zr(\mu\text{-H})_3(AlBu^i_2)_2(\mu\text{-Cl})$ (**6b**)	220	−1.75 (d, 4.8 Hz, 2H) −0.67 (t, 7.2 Hz, 1H)	5.87 (m, 8H, CH) 5.45 (m, 8H, CH) 1.72 (s, 6H, CH_3)
$Ind_2Zr(\mu\text{-H})_3(AlBu^i_2)_2(\mu\text{-Cl})$ (**6f**)	220	−1.11 (d, 5.6 Hz, 2H) 0.07 (t, 7.6 Hz, 1H)	7.37 (m, 4H, CH) 6.87 (m, 4H, CH) 6.32 (m, 2H, CH) 5.19 (m, 4H, CH)
$Me_2Si(Ind)_2Zr(\mu\text{-H})_3(AlBu^i_2)_2(\mu\text{-Cl})$ (**6h**)	220	−1.55 (m, 2H) 1.06 (m, COSY)	7.85 (d, 7.6 Hz, 2H, CH) 7.39 (m, CH, COSY) 6.83 (m, CH, COSY) 6.92 (m, 4H, CH) 5.81 (m, 2H, CH) 0.52 (NOESY, $SiMe_3$)
$C_2H_4(Ind)_2Zr(\mu\text{-H})_3(AlBu^i_2)_2(\mu\text{-Cl})$ (**6i**)	220	−1.00 (m, 2H) 0.62 (m, COSY)	7.43 (d, 8.8 Hz, 2H, CH) 7.15 (m, CH, COSY) 6.89 (m, 2H, CH) 6.81 (m, 2H, CH) 6.40 (m, 2H, CH) 5.75 (m, 2H, CH) 2.65, 3.05 (m, NOESY, $-CH_2CH_2-$)
$(C_5Me_5)_2ZrH(\mu\text{-H})_2(AlBu^i_2)_2(\mu\text{-Cl})$ (**5c**)	220	−1.27 (m, 1H) −0.66 (d, 9.6 Hz, 1H) 4.38 (dd, 9.6 Hz, 4.0 Hz, 1H) (Zr−H)	1.99 (s, 30H, CH_3)
rac-$Me_2C(2\text{-Me-4-Bu}^t\text{-}C_5H_2)_2ZrH(\mu\text{-H})_2(AlBu^i_2)_2(\mu\text{-Cl})$ (**5d**)	195	−0.91 (m, 1H) −0.33 (m, 1H) 2.28 (m, COSY) (Zr−H)	6.69 (m, 1H, CH) 6.35 (m, 1H, CH) 4.88 (m, 1H, CH) 4.80 (m, 1H, CH)
meso- $Me_2C(2\text{-Me-4-Bu}^t\text{-}C_5H_2)_2ZrH(\mu\text{-H})_2(AlBu^i_2)_2(\mu\text{-Cl})$ (**5e**)	300	−1.07 (m, 1H) 1.19 (m, COSY) 3.51 (m, COSY) (Zr−H)	5.67 (d, 2.4 Hz, 2H, CH) 4.94 (m, 2H, CH) 2.22 (s, 6H, CH_3) 1.58 (m, 3H, CH_3) 1.30 (m, 3H, CH_3) 1.33 (m, 18H, CH_3)
rac-$Me_2C(3\text{-Bu}^t\text{-}C_5H_2)_2ZrH(\mu\text{-H})_2(AlBu^i_2)_2(\mu\text{-Cl})$ (**5f**)	194	−0.94 (m, 1H) −0.78 (m, 1H) 2.05 (m, COSY) (Zr−H)	6.66 (m, 1H, CH) 6.45 (m, 1H, CH) 5.77 (m, 1H, CH) 5.54 (m, 1H, CH) 4.86 (m, 1H, CH) 4.53 (m, 1H, CH)
$(C_5H_5)_2Zr(\mu\text{-H})_3(AlBu^i_2)_3(\mu\text{-Cl})(\mu\text{-H})$ (**8a**)	220	−3.05 (m, 1H) −2.30 (m, 1H) −1.22 (m, 1H) 3.56 (m, 1H) (Al−H−Al)	5.66 (s, 10H)
$(C_5H_4Me)_2Zr(\mu\text{-H})_3(AlBu^i_2)_3(\mu\text{-Cl})(\mu\text{-H})$ (**8b**)	220	−2.54 (m, 1H) −1.75 (m, 1H) −0.85 (m, 1H) 3.71 (m, 1H) (Al−H−Al)	6.09 (m, 2H, CH) 5.87 (m, 2H, CH) 5.52 (m, 2H, CH) 5.37 (m, 2H, CH) 1.76 (s, 6H, CH_3)
$(C_5H_5)_2Zr(\mu\text{-H})_3(AlBu^i_2)_3(\mu\text{-Cl})_2$ (**10a**)	220	−2.27 (m, 2H) −1.04 (m, 1H)	5.68 (s, 10H)
$(C_5H_5)_2Zr(\mu\text{-H})_3(AlBu^i_2)(AlBu^i_3)$ (**16a**)	230	−2.48 (m, 1H) −1.83 (d, 7.6 Hz, 1H) −1.15 (d, 6.4 Hz, 1H)	5.56 (s, 10H)
$(C_5H_5)_2Zr(\mu\text{-H})_3(AlEt_2)_2(\mu\text{-Cl})$ (**19b**)	293	−0.71 (br s, 1H) −1.68 (br s, 2H)	5.68 (m, 8H, CH) 5.44 (m, 8H, CH) 1.73 (s, 6H, CH_3)
$(C_5H_5)_2Zr(\mu\text{-H})_3(AlBu^i_2)_3(\mu\text{-H})_2$ (**20a**)	210	−2.20 (d, 15.2 Hz, 2H) −1.34 (t, 15.2 Hz, 1H) 3.28 (br s, 2H) (Al−H−Al)	5.45 (s, 10H)

Table 1. continued

$^a\delta$ values given in ppm at 400.13 MHz in d_8-toluene.

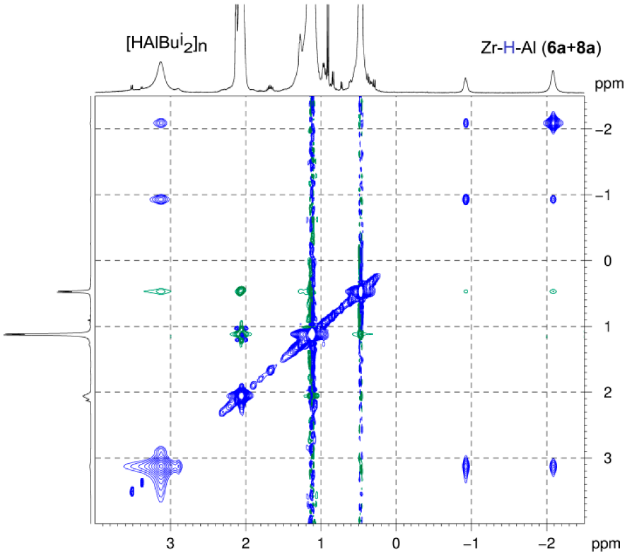

Figure 6. EXSY spectrum of the system $(C_5H_5)_2ZrCl_2$ (**1a**)−$HAlBu^i_2$ (1:3) in d_8-toluene at 290 K (τ = 0.3 s).

Scheme 4

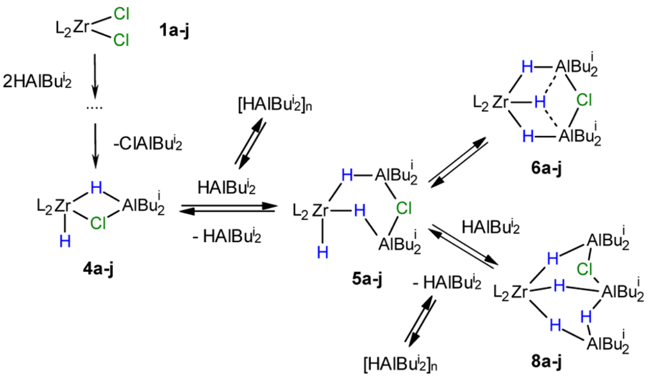

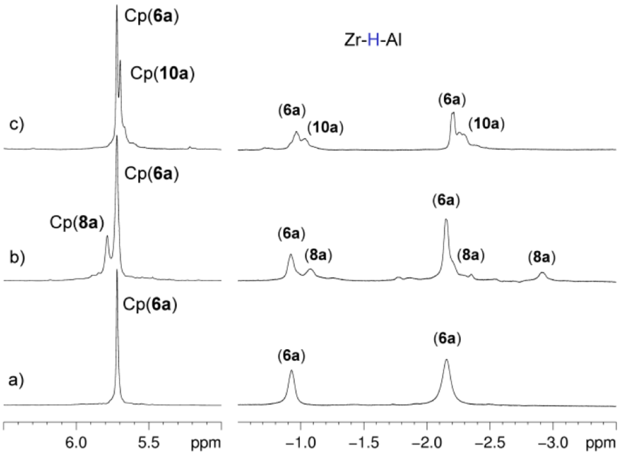

Figure 7. ^{1}H NMR of complex **6a** (a), **6a** + $ClAlBu^i_2$ (b), and **6a** + $HAlBu^i_2$ (c) in C_7D_8 at 220 K (the intensity of upfield signals is increased for clarity).

Scheme 5

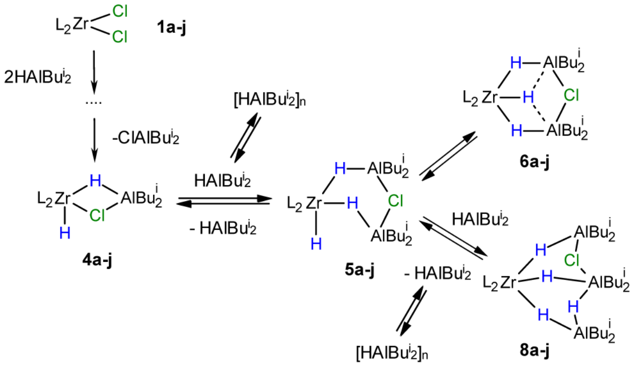

temperature range from 209 to 282 K fully corresponded to structure **6a**, resulting from the reaction of **1a** with $HAlBu^i_2$ (Scheme 4).

However, the molecular mass of the compound determined by cryoscopy in benzene proved to be lower than the theoretical value (541 g/mol) and was equal to 487 ± 11 g/mol. The addition of $HAlBu^i_2$ to complex **6a** obtained by the alternative synthesis gives rise to ^{1}H NMR signals of compound **8a** (Figure 7 and Scheme 5). However, in this case no agreement between the theoretical and experimental molecular masses of the complex was observed as well (M_{exptl} = 529 ± 10 g/mol, $M_{\text{theor.}}$= 684 g/mol). Meanwhile, the addition of $ClAlBu^i_2$ to **6a** gives rise to downfield signals in the low-temperature ^{1}H NMR spectra corresponding to the cyclopentadienyl ligands and the hydride atoms of a new complex, which contains the $[(C_5H_5)_2ZrH_3]$ moiety as well and is very similar to **6a** (Figure 7); hence, structure **10a** was ascribed to the new complex. In this case, the molecular mass did not increase significantly either, being 533 ± 15 g/mol (M_{theor} = 718 g/mol). A temperature rise to 300 K induces coalescence of the signals for cyclopentadienyl groups and bridging hydride atoms of **6a** and **10a**, indicating the existence of fast intermolecular exchange between them. Apparently, the lower molecular masses found for complexes **6a**, **8a**, and **10a** by the cryoscopic method in comparison to the theoretical values are due to the fact that these compounds tend to dissociate and exist in equilibrium with other Zr,Al-hydride complexes and OAC oligomers.

Additionally, we investigated the complex $(C_5H_5)_2Zr(\mu\text{-}H)_3(AlBu^i_2)_3(\mu\text{-}H)_2$ (**9a**), which was postulated to form in the **1a**−$HAlBu^i_2$ system in our previous studies[6,9] and was detected[8] in the reaction of 1/2 equiv of $[(C_5H_5)_2ZrH_2]_2$ with 3 equiv of $HAlBu^i_2$. We found that complex **9a** is actually observable in this reaction at temperatures below 240 K (Scheme 5 and Figures S5 and S6 in the Supporting Information). The EXSY spectra at 240 K exhibit the hydride exchange both within the complex molecules and with $[HAlBu^i_2]_n$ oligomers (Figure S8 in the Supporting Information). Molecular mass determination (cryoscopy in benzene) for the presumed cluster **9a** does not confirm the existence of this species, at least above 0 °C ($M_{\text{exptl.}}$= 378 ± 27 g/mol, $M_{\text{theor.}}$= 649 g/mol). Thus, at room temperature, complex **9a**, like **6a**, **8a**, and **10a**, exists in a fast exchange with smaller clusters, for example, **13a** and **14a**, and oligomers $[HAlBu^i_2]_n$.

The obtained NMR data indicate unambiguously that complex **9a** is not formed in the **1a**−HAlBu$^{i}_{2}$ system.

Further, the reactivity of complexes **6a** and **8a**−**10a** with respect to alkenes was studied. Earlier, we considered complex **6a** to be nonreactive, because the addition of alkene to this complex in the NMR tube did not produce any visible changes in the ^{1}H NMR spectrum over a 1 h period. Studies in a magnetically stirred solution demonstrated (Figure 8) that **6a** reacts with a terminal alkene quite slowly, so that 92% conversion of the alkene is achieved only in 19 h. The addition of 1 equiv of ClAlBu$^{i}_{2}$ or HAlBu$^{i}_{2}$ to **6a** induces a slight decrease in the reaction rate due to an equilibrium shift toward complex **8a** or **10a**, which should be less reactive in hydroalumination according to theoretical data.[6,9] However, in this case 77−80% conversion of the alkene was noted after 15−20 h of the reaction. Complex **9a** proved to be somewhat more reactive than **6a** during the first 3 h of the reaction, but finally, after 19 h, the yield of the hydroalumination product was in the same range as the yields of the reactions involving complexes **6a**, **8a**, and **10a**.

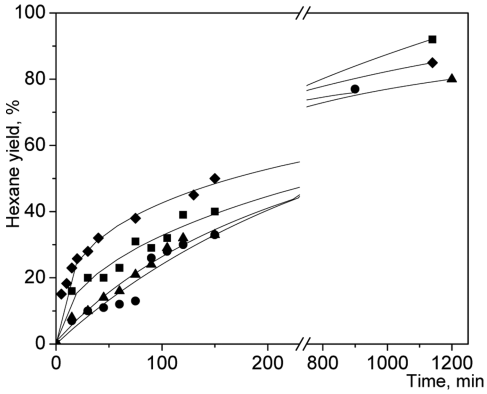

Figure 8. Yield of hydrometalation product in the reaction of hexene-1 with complexes **6a** (■), **8a** (**6a** + HAlBu$^{i}_{2}$) (▲), **10a** (**6a**+ ClAlBu$^{i}_{2}$) (●), and **11a** (♦) (C_6H_6, t = 22 °C).

The low-temperature NMR study of the reaction of **1a** with AlBu$^{i}_{3}$ at a ratio of 1:4.5 demonstrated the initial formation of alkyl chloride complex **15a**,[4] which was then converted to compounds **16a** and **6a** upon isobutylene elimination (Scheme 6 and Figure S9 in the Supporting Information). The structure of complex **16a** was identified on the basis of three doublets for magnetically nonequivalent hydride atoms of the Zr−H−Al bridging bonds in a 1:1:1 ratio present in the high-field region (δ_H −1.15, −1.83, and −2.48) of the low-temperature (230 K) ^{1}H NMR spectrum (Table 1). A temperature increase induced coalescence of the signals for cyclopentadienyl ligands of complexes **16a** and **6a** and broadening of signals for the bridging hydride atoms. The addition of ClAlBu$^{i}_{2}$ to a mixture of the complexes increased the content of **6a**. In the EXSY spectra recorded in the temperature range 260−280 K we detected slow intermolecular exchange of hydrides between particular types of the Zr−H−Al bonds in **16a** and **6a**: namely, the signals for internal atoms and the signals for external atoms exchanged in pairs (Figure 9b). The observed fact may be a consequence of the exchange of AlBu$^{i}_{3}$ and ClAlBu$^{i}_{2}$ molecules between **16a** and **6a** via partial dissociation of the bimetallic clusters to give complex **13a** (Scheme 6). In this system the dynamic processes have a lower rate in comparison with the **1a**−HAlBu$^{i}_{2}$ system; this is indicated by the higher minimum temperature at which the slow exchange can be detected. Apparently, the absence of fast exchange between the hydride clusters, resulting in longer lifetimes of intermediates with a free Zr−H bond and the lack of possibility of formation of larger clusters, is the reason for the high reactivity of the **1a**−AlBu$^{i}_{3}$ catalytic system toward alkenes.

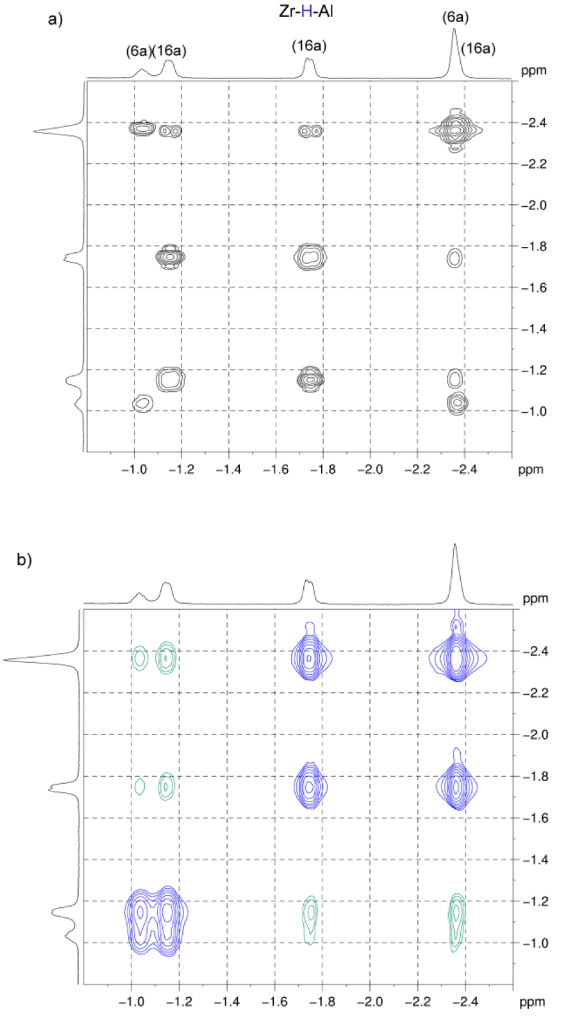

Figure 9. Upfield region of COSY (a) and EXSY (b) spectra of the system $(C_5H_5)_2ZrCl_2$ (**1a**)−AlBu$^{i}_{3}$ (1:4.5) in d_8-toluene at 270 K.

Scheme 6

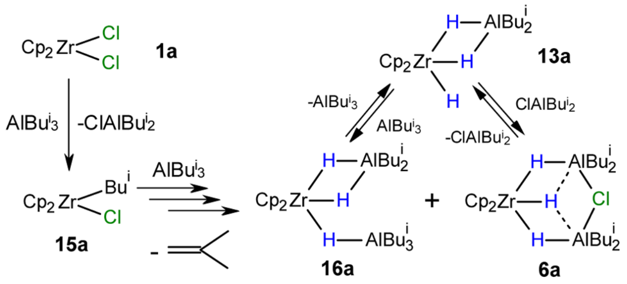

B. System Based on the C_5H_4Me Ligand. The NMR spectra recorded during the reaction of $(C_5H_4Me)_2ZrCl_2$ (**1b**) with HAlBu$^{i}_{2}$ (1:5) showed, apart from the initial OAC, the presence of complexes **6b** and **8b**, similar to the case for the cyclopentadienyl analogues, in a 3.4:1 ratio (Table 1 and

Figure S10 in the Supporting Information). Here, as in the case of the bimetallic cyclopentadienyl complexes, the hydride exchange occurs within the complexes, between the complexes, and between the complexes and $HAlBu^i_2$ oligomers (Figure S13 in the Supporting Information). The constants and the activation parameters of **6b** ↔ **8b** exchange correspond to those for **6a** ↔ **8a**: namely, $k_{220} = 12.0$ s^{-1}, $\Delta G^{\ddagger}_{220} = 11.94 \pm 0.04$ kcal/mol, $\Delta H^{\ddagger} = 6.19 \pm 0.40$ kcal/mol, and $\Delta S^{\ddagger} = -25.94 \pm 7.52$ cal/(mol K).

It is noteworthy that in an attempt to synthesize complexes **7b** or **17b**, analogues of the cyclopentadienyl complex prepared in our earlier works,[4,5] by the reaction of $[(C_5H_4Me)_2ZrH_2]_2$ (**12b**) with $ClAlR_2$ (R = Et, Bu^i) at 20 °C in benzene or toluene was not successful. Instead of the expected **7b** (**17b**), the reaction provided trihydride complexes **6b** (**19b**) (Scheme 7).

Scheme 7

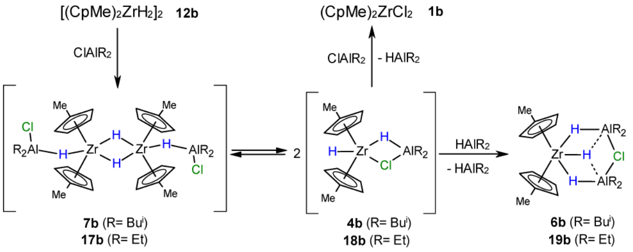

According to monitoring of this reaction directly in the NMR spectrometer cell, along with the complexes **6b** (**19b**) formed, the mixture contained both the starting **12b** and **1b**. Probably, complex **7b** (**17b**) formed in the first step rapidly react swith $ClAlR_2$ via monomer **4b** (**18b**), giving rise to **1b** and to elimination of $HAlR_2$. The latter reacts with intermediate **4b** (**18b**), providing the complex **6b** (**19b**). The structures of complexes **6b**,**c** proved to be similar to the structure of complex **6a** described above.

Upon the addition of alkene (1-hexene) to the **1b**–$HAlBu^i_2$ reaction mixture in an NMR tube at room temperature, signals for the complex $(C_5H_4Me)_2Zr(n\text{-}C_6H_{13})Cl$ and $RAlBu^i_2$[4] (**2**) appear in the ^1H and ^{13}C NMR spectra (Figures S17 and S18 in the Supporting Information). Alkylalane $RAlBu^i_2$ forms the associates $RAlBu^i_2 \cdot HAlBu^i_2$[17] in the presence of excess $HAlBu^i_2$, according to ^1H NMR data (the signal of the monomeric associated $HAlBu^i_2$ occurs at δ_H 3.97 ppm).

C. Systems Based on Indenyl Ligands. The NMR spectra of the reaction mixture Ind_2ZrCl_2 (**1g**)–$HAlBu^i_2$ (1:12) at 300 K contained one broadened signal for hydride atoms at −0.94 ppm, the ratio of which with the resonance lines of the indenyl ligand attested to the formation of a complex containing a $[L_2ZrH_3]$ moiety. Lowering the temperature to 280 K and below gave rise to two upfield signals: a broadened triplet at δ_H 0.05 ppm and a doublet at δ_H −1.04 ppm with an intensity ratio of 1:2 (Table 1). The downfield part of the spectrum displayed two signals for cyclopentadienyl protons of the indenyl ligand: a triplet at δ_H 6.35 and a doublet at δ_H 5.31 ppm. The intensity ratio of the four aforementioned signals was 1 (Zr–H–Al):2 (Zr–H–Al):2 (Ind):4 (Ind). A decrease in the temperature to 220 K did not result in considerable changes in the shape of the signals for hydride and indenyl hydrogens. Hence, the complex was identified as structure **6g**. The EXSY spectra at 280 K exhibited cross-peaks corresponding to the exchange of the hydride atoms between the bridging Zr–H–Al bonds and the trimer $HAlBu^i_2$ (Figure 10).

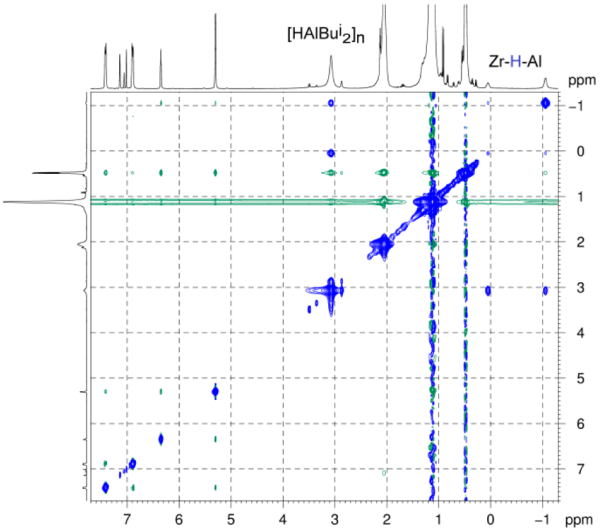

Figure 10. EXSY spectrum of the system Ind_2ZrCl_2 (**1g**)–$HAlBu^i_2$ (1:12) in d_8-toluene at 275 K (τ = 0.3 s).

In the case of *rac* complexes containing *ansa*-bonded indenyl ligands (**1i**,**j**), we observed almost the same pattern as for **1g** (Figures S35–S42 in the Supporting Information). The intermediates detected at 220 K were also identified as being trihydride clusters **6i**,**j** with bridging Zr–H–Al bonds (Table 1). This assignment is supported by the absence of additional splitting of the proton signals of the *ansa* ligands, which would inevitably appear upon generation of the stereogenic center on Zr if nonsymmetric complexes **5i**,**j** or **8i**,**j** were formed.

The system showed low activity toward terminal alkenes. The formation of hydroalumination products was observed no earlier than 2 h after placement of the alkene directly in the NMR tube.

D. Systems Based on Sterically Hindered Cp Ligands. The reaction of $(C_5Me_5)_2ZrCl_2$ (**1c**) with $HAlBu^i_2$ gives a complex containing a $[L_2ZrH_3]$ moiety. Thus, the ^1H NMR spectrum of a **1c** + $HAlBu^i_2$ mixture (1:26) at temperatures below 280 K exhibited, apart from the lines for the remaining initial complex **1c**, a signal for the hydride atom of the terminal Zr–H bond at δ_H 4.38 ppm, which was correlated in the COSY spectra with upfield signals at δ_H −0.66 and −1.27 ppm (Figure S16 in the Supporting Information). The integral intensity ratio for these signals was 1:1:1 (Table 1). A temperature increase to 300 K induced broadening of the hydride signals, which finally ceased to be detected in the spectra (Figure S15 in the Supporting Information).

Complexes **5c**, **13c**, and **20c** could be proposed as the possible structures of the observed intermediate (Scheme 8). In view of the fact that these complexes are prone to form tri- and tetrametallic clusters, the existence of **13c** is unlikely. Structure **20c** was not detected, because the spectra did not exhibit proton signals for the bridging Al–H–Al bond. Therefore, the observed intermediate can most likely be described as **5c**.

The EXSY spectra recorded at 265 K prove the existence of exchange between the hydride atoms within complex **5c** and the exchange of these hydrides with $[HAlBu^i_2]_n$ oligomers. Moreover, in the spectra we found cross-peaks between the signals of $[HAlBu^i_2]_n$ hydrides and the downfield broadened signal at 6.85 ppm (Figure 11), which can be attributed to the hydride atoms of free $(CMe_5)_2ZrHCl$[18] (**3c**). Apparently, the existence of uncomplexed zirconocene hydride in the system is

Scheme 8

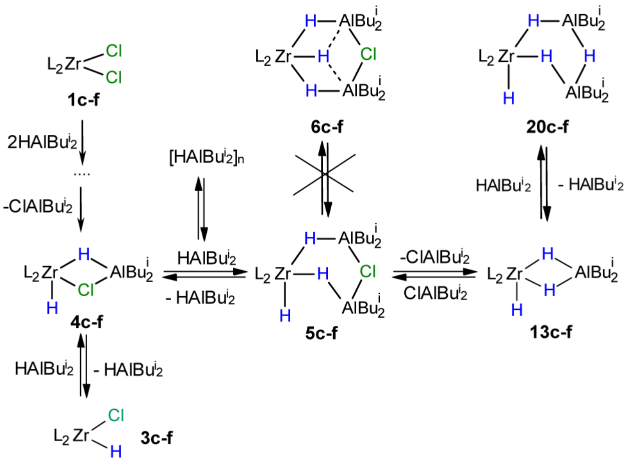

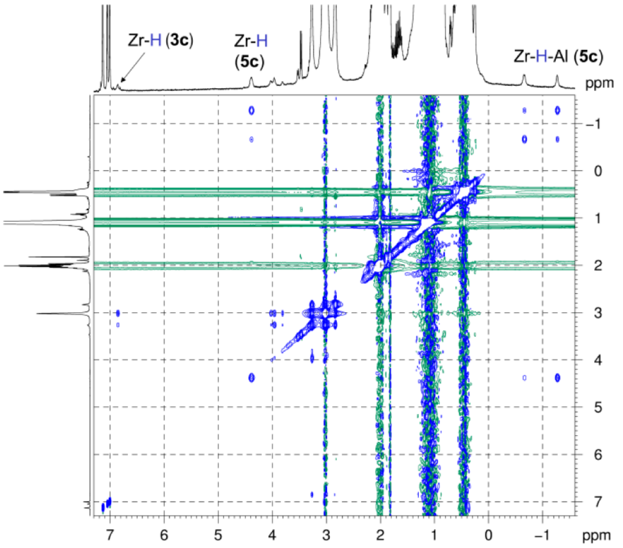

Figure 11. EXSY spectrum of the system (CMe$_5$)$_2$ZrCl$_2$ (**1c**)−HAlBu$^i_2$ (1:26) in d_8-toluene at 265 K (τ = 0.3 s).

caused by the tendency of the bimetallic clusters to dissociate due to the steric hindrance in the η^5 ligand.

A more complex pattern is observed in the reaction of sterically hindered *ansa*-bonded cyclopentadienyl *rac* complexes **1d,f** with HAlBu$^i_2$. The ^{1}H NMR spectrum of the **1d** + HAlBu$^i_2$ system (1:17) recorded at 230 K showed two broadened signals in the downfield region for the protons of bound bis-cyclopentadienyl ligand (δ_H 6.52 and 4.90 ppm) and a broadened signal for the bridging hydride atoms in a upfield region (δ_H −0.58 ppm). The signal ratio was 1:1:1 (Table 1). This situation occurred in the temperature range from 230 to 280 K. In the COSY spectra, the signal at δ_H −0.58 ppm was correlated with the signal at δ_H 2.28 ppm, which can be assigned to the terminal hydride atom at Zr. In the EXSY spectra recorded at 260−270 K, we detected cross-peaks corresponding to the slow exchange of two hydride atoms at δ_H −0.58 and 2.28 ppm and the exchange of these hydride hydrogens with the [HAlBu$^i_2$]$_n$ oligomers (Figure S21 in the Supporting Information). A further temperature increase induced pronounced line broadening for both hydride bridge and ligand proton signals (Figure 12). Finally, at 300 K, some of these lines were no longer detected in the spectra. The temperature decrease from 230 to 195 K caused additional splitting into halves of the downfield signals for the ligand protons and the upfield signal for the bridging hydride atoms.

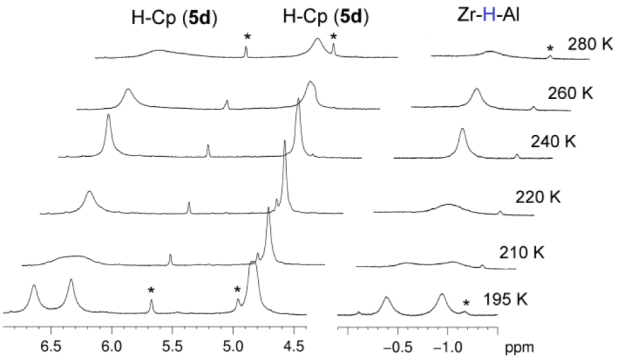

Figure 12. Variable-temperature ^{1}H NMR study on the system *rac*-Me$_2$C(2-Me-4-Bu^t-C$_5$H$_2$)$_2$ZrCl$_2$ (**1d**)−HAlBu$^i_2$ (1:17) in C$_7$D$_8$ (asterisks indicate an admixture of *meso* isomer).

These results can be interpreted in the following way. The NMR spectral pattern observed at 230−280 K contributes to the existence of a structure with the [L$_2$ZrH$_3$] moiety containing a terminal Zr−H bond. Thus, in the case of formation of open structures such as **5$_1$d**−**5$_4$d** (**5$_1$d**−**5$_3$d** and **5$_2$d**−**5$_4$d** are enantiomer pairs), the spectra should exhibit four signals for H^1−H^4 protons of the cyclopentadienyl groups of the *ansa* ligand, which are expected to be magnetically nonequivalent upon reduction of the symmetry of the complex (Scheme 9). This corresponds to the NMR spectral pattern at temperatures below 210 K; this is apparently manifested due to slowing of the hydride exchange in the complex. The H^2−H^4 and H^1−H^3 proton exchange observed as the temperature is raised can be attributed to intramolecular rearrangement of the terminal and bridging bonds in **5$_1$d** ↔ **5$_2$d** and in their enantiomers **5$_3$d** ↔ **5$_4$d**. At temperatures above 230 K, a substantial contribution is made by the intermolecular exchange with dissociation of the bridging Zr−H−Al bonds and elimination of OAC molecules, as indicated by the data of the EXSY spectra.

Scheme 9

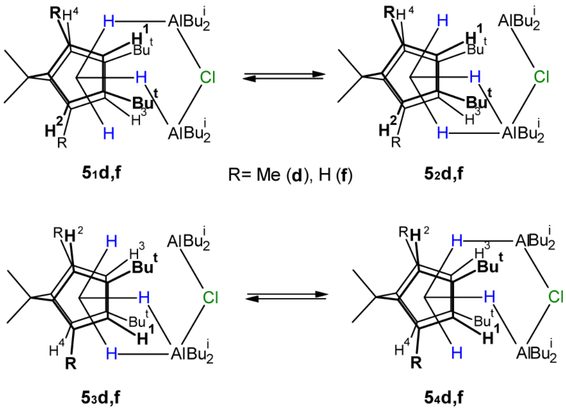

A similar situation was observed for the **1f** + HAlBu$^i_2$ system (1:13). In this case, the low-temperature spectra exhibited an additional pair of signals for the third proton of the cyclopentadienyl moieties of the *ansa* ligands in the intermediate **5f** (Figures S28 and S29 in the Supporting Information).

Upon the addition of alkene to the reaction mixture in the NMR tube, the reaction occurred almost instantaneously: the signals for the intermediate hydride atoms and η^5 ligand disappeared, and simultaneously the ^{1}H and ^{13}C NMR spectra started to exhibit resonance lines for $RAlBu^i_2 \cdot HAlBu^i_2$.

A somewhat different situation was observed in the reaction of $HAlBu^i_2$ with *meso* isomer **1e**. As in the case of **1c**,**d**,**f**, the ^{1}H NMR spectra of the reaction mixture contained signals for the terminal hydride atom at δ_H 3.51 ppm and signals for bridging hydrides at δ_H 1.19 and −1.07 ppm, which can be attributed to structure **5e** (Scheme 10). The temperature variation did not induce a change in the signal shape, and the EXSY spectra did not show cross-peaks characteristic of hydride exchange; this implies the absence of both intra- and intermolecular dynamic processes. According to NOESY spectra, the terminal hydride H_α atom occurs in the close vicinity of the Bu^t groups and the H^2 protons of the *ansa* ligand. This shielding precludes association of this hydride with the organoaluminum moiety, which probably terminates both the intramolecular exchange between the possible structures **5e** ↔ **5e**′ and the intermolecular exchange **5e** ↔ $[HAlBu^i_2]_n$.

Scheme 10

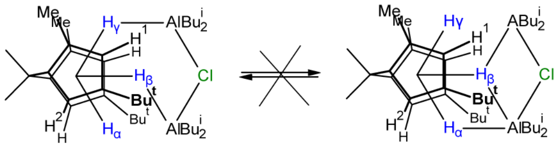

The observed complex **5e** did not react with the alkene: according to NMR data, no signs of reaction were observed even after 24 h. This may also be due to the ligand steric influence, which prevents the substrate coordination to the terminal Zr−H bond in complex **5e**.

In the reaction of **1c**−**f** with $ClAlBu^i_2$ or $AlBu^i_3$, the alkyl chloride ligand exchange was not manifested in the NMR spectra. Moreover, if one assumes that this exchange occurs in a catalytic version, the rate of formation of the key hydride intermediates via C−H activation in the isobutyl group and isobutene elimination from the alkylzirconocene complex should be very low[19] due to the presence of sterically hindered η^5 ligands in the molecule. Apparently, the low rate of these two steps is responsible for the low catalytic activity of complexes **1c**−**f** in the alkene hydroalumination with $ClAlBu^i_2$ ($AlBu^i_3$) (Figure 1d).

■ CONCLUSION

Studies on the catalytic activity of the systems L_2ZrCl_2−$XAlBu^i_2$ (L = C_5H_5, C_5H_4Me, Ind, C_5Me_5; L_2 = *rac*-$Me_2C(2\text{-}Me\text{-}4\text{-}Bu^t\text{-}C_5H_2)_2$, *meso*-$Me_2C(2\text{-}Me\text{-}4\text{-}Bu^t\text{-}C_5H_2)_2$, *rac*-$Me_2C(3\text{-}Bu^t\text{-}C_5H_3)_2$, *rac*-$Me_2C(Ind)_2$, *rac*-$Me_2Si(Ind)_2$, *rac*-$C_2H_4(Ind)_2$); X = H, Cl, Bu^i) in the alkene hydroalumination showed that the maximum effect was attained by using complexes with more sterically crowded cyclopentadienyl ligands in combination with $HAlBu^i_2$. Catalysts with less bulky ligands are the most active in the reaction of alkenes with $AlBu^i_3$ or $ClAlBu^i_2$. The indenyl zirconium complexes provide a considerable decrease in the yield of the hydroalumination products irrespective of the OAC structure.

The observed dependence of the catalytic system activity on the OAC nature and the ligand structure in the zirconocene is related to the structural and dynamic features of the bimetallic hydride intermediates formed in these systems. It was shown that the use of catalysts with less electron donating and sterically crowded ligands leads to the formation of the stable Zr,Al-hydride clusters $L_2Zr(\mu\text{-}H)_3(AlBu^i_2)_2(\mu\text{-}Cl)$ (L = C_5H_5, C_5H_4Me, Ind; L_2 = *rac*-$Me_2C(Ind)_2$, *rac*-$Me_2Si(Ind)_2$, *rac*-$C_2H_4(Ind)_2$), $L_2Zr(\mu\text{-}H)_3(AlBu^i_2)_3(\mu\text{-}Cl)(\mu\text{-}H)$, and $L_2Zr(\mu\text{-}H)_3(AlBu^i_2)_3(\mu\text{-}Cl)_2$ (L = C_5H_5, C_5H_4Me), which tend to form bridging Zr−H−Al bonds; hence, these complexes have low activity in the reaction with alkene. We also found intra- and intermolecular exchange between the hydride atoms in these clusters and $[HAlBu^i_2]_n$ oligomers. As a result, the complexes exist in equilibrium with each other and $HAlBu^i_2$ self-associates, while the intermolecular exchange involves the OAC monomer and occurs via dissociation of bimetallic complexes. As the $[HAlBu^i_2]_n$ concentration increases, i.e., the reaction approaches the catalytic version, the equilibrium shifts toward large clusters of low activity in which the alkene insertion is hampered due to the competing intermolecular exchange with OAC oligomers.

In the reaction of $AlBu^i_3$ with $(C_5H_5)_2ZrCl_2$, alkyl chloride exchange and isobutylene elimination give the intermediates $(C_5H_5)_2Zr(\mu\text{-}H)_3(AlBu^i_2)(AlBu^i_3)$ and $(C_5H_5)_2Zr(\mu\text{-}H)_3(AlBu^i_2)_2(\mu\text{-}Cl)$, which exist with intermolecular exchange of $AlBu^i_3$ and $ClAlBu^i_2$ groups. The absence of fast exchange between these hydride clusters increases the lifetime of the active sites with free Zr−H bonds, and this is responsible for the high activity of the $(C_5H_5)_2ZrCl_2$−$AlBu^i_3$ catalytic system toward alkene.

In the reactions catalyzed by Zr complexes with bulky ligands (L = C_5Me_5, *rac*-$Me_2C(2\text{-}Me\text{-}4\text{-}Bu^t\text{-}C_5H_2)_2$, *rac*-$Me_2C(3\text{-}Bu^t\text{-}C_5H_3)_2$), Zr,Al-bimetallic active sites containing a $[L_2ZrH_3]$ moiety with a free Zr−H bond are formed, and the steric hindrance in the ligand prevents the formation of low-activity intermediates; therefore, high yields of hydroalumination products are achieved. The *meso* isomer of the sterically hindered cyclopentadienyl complex $Me_2C(2\text{-}Me\text{-}4\text{-}Bu^t\text{-}C_5H_2)_2ZrCl_2$ gives an intermediate with a shielded free Zr−H bond, which makes the catalytic system inactive.

Finally, the L_2ZrCl_2−$XAlBu^i_2$ systems can be classified as labile systems in which intra- and intermolecular hydride exchange between Zr and Al, controlled by the steric factor of the η^5 ligand, OAC nature, and the reaction conditions (reactant ratio), plays the key role in the catalytic process.

■ EXPERIMENTAL SECTION

General Procedures. All operations were carried out under argon using Schlenk techniques. Solvents were dried by refluxing over $HAlBu^i_2$ and freshly distilled prior to use. The commercial organoaluminum compounds $HAlBu^i_2$ (99%, Aldrich), $ClAlBu^i_2$ (97%, Strem), $ClAlEt_2$ (97%, Strem), and $AlBu^i_3$ (95%, Strem) were used in the reactions. *Caution! The pyrophoric nature of aluminum alkyl and hydride compounds requires special safety precautions in their handling.* The complexes $(C_5H_5)_2ZrCl_2$ (**1a**),[20] $(C_5H_4Me)_2ZrCl_2$ (**1b**),[21] Ind_2ZrCl_2 (**1g**),[22] $Me_2C(Ind)_2ZrCl_2$ (**1h**),[23] *rac*-$Me_2C(2\text{-}Me\text{-}4\text{-}Bu^t\text{-}C_5H_2)_2ZrCl_2$ (**1d**) (contains ~7% of **1e**),[10g] *meso*-$Me_2C(2\text{-}Me\text{-}4\text{-}Bu^t\text{-}C_5H_2)_2ZrCl_2$ (**1e**) (contains ~17% of **1d**),[10g] and *rac*-$Me_2C(3\text{-}^tBu\text{-}C_5H_3)_2ZrCl_2$ (**1f**)[10g] were synthesized from $ZrCl_4$ (Aldrich, 99.5%). Zirconocenes $(C_5Me_5)_2ZrCl_2$ (**1c**; 97%, Acros), *rac*-$Me_2Si(Ind)_2ZrCl_2$ (97%, Strem), and *rac*-$C_2H_4(Ind)_2ZrCl_2$ (Strem) were purchased and used as received. The synthesis of $[(C_5H_5)_2ZrH_2]_2$ and $[(C_5H_4Me)_2ZrH_2]_2$ from the corresponding zirconocene dichlorides was performed as described previously.[7,4]

The ^{1}H and ^{13}C NMR spectra were recorded on a Bruker AVANCE-400 spectrometer (400.13 MHz (^{1}H), 100.62 MHz (^{13}C)).

DOI: 10.1021/acs.organomet.5b00370
Organometallics XXXX, XXX, XXX−XXX

Toluene-d_8 and benzene-d_6 were employed as the solvents and internal standards. 1D and 2D NMR spectra (COSY HH, HSQC, HMBC, EXSY (NOESY)) were recorded using standard Bruker pulse sequences. The constants and activation parameters of intermediate exchange were found using line shape analysis of NMR spectra with the program Bruker TopSpin 3.0.

The hydrolysis products of reaction mixtures were analyzed on a Chrom-5 chromatograph (flame ionization detector, 2 m × 3 mm column, 15% Peg-6000, 50–190 °C).

The cryoscopic measurements were carried out in benzene by a standard procedure[24] in a glass cell equipped with a Beckmann thermometer (the accuracy of melting point determinations was 0.005 °C).

Study of the Catalytic Activity of L_2ZrCl_2 in the Reaction of $XAlBu^i_2$ with Alkenes. A flask with a magnetic stirrer was filled under argon with **1a–j** (0.20 mmol), 1-alkene (10 mmol), 3 mL of benzene, and OAC (12 mmol). The reaction was carried out with stirring. At specific time intervals, samples (0.2 mL) of the reaction mixture were syringed into tubes filled with argon, and then the samples were treated with 10% HCl at 0 °C. The products were extracted with benzene, and the organic layer was dried above Na_2SO_4. The yield of alkylalanes was determined via the amount of hydrolysis products of the reaction mixture (alkane relative to initial terminal alkene) by GLC.

NMR Study of Intermediate Structures in the Reaction of L_2ZrCl_2 (1a–j) with $XAlBu^i_2$ (X = H, Cl, Bu^i). An argon-filled NMR tube was charged with 0.03–0.04 mmol of L_2ZrCl_2 (**1a–j**), 0.4 mL of toluene-d_8, and 0.14–0.90 mmol of $XAlBu^i_2$. The mixture was stirred and, after 30 min, transferred into the spectrometer cavity to record the spectra in the temperature range from 300 to 190 K.

Reaction of $[(C_5H_5)_2ZrH_2]_2$ with $HAlBu^i_2$. An NMR tube was charged with 0.05 mmol (22.2 mg) of $[(C_5H_5)_2ZrH_2]_2$ (**12a**) and 0.3 mL of toluene-d_8 in an argon-filled glovebox. Then the mixture was cooled to 240 K and 0.3 mmol of $HAlBu^i_2$ was added dropwise until complete dissolution of precipitate. The mixture was stirred, and the tube was introduced into the NMR probe to record the spectra in the temperature range from 300 to 190 K. Complex **9a** was identified in the mixture at temperatures below 240 K.

Reaction of $[(C_5H_5)_2ZrH_2]_2$ with $ClAlBu^i_2$ and $HAlBu^i_2$. An NMR tube was charged with 0.05 mmol (22.2 mg) of $[(C_5H_5)_2ZrH_2]_2$ (**12a**) and 0.3 mL of toluene-d_8 in an argon-filled glovebox. The mixture was cooled to 220 K, and 0.1 mmol of $ClAlBu^i_2$ was added dropwise until complete dissolution of precipitate. Then 0.1 mmol of $HAlBu^i_2$ was added. The tube was introduced into the NMR probe, and the formation of complex **6a** was monitored at 210–220 K. Further addition of extra amounts of $ClAlBu^i_2$ or $HAlBu^i_2$ (0.1 mmol) provided mixtures of complexes **6a** + **10a** or **6a** + **8a**, respectively, as determined from low-temperature NMR spectra.

Reaction of $[(C_5H_4Me)_2ZrH_2]_2$ with $ClAlR_2$. An NMR tube was charged with 0.05 mmol (25.1 mg) of $[(C_5H_4Me)_2ZrH_2]_2$ (**12b**) and 0.3 mL of toluene-d_8 in an argon-filled glovebox. Then the mixture was cooled to 220 K and 0.1 mmol of $ClAlR_2$ (R = Bu^i, Et) was added dropwise. The mixture was stirred, and the tube was introduced into the NMR probe to record the spectra in the temperature range from 300 to 190 K. Complexes **1b** and **6b** (**19b**) were identified in the mixture.

■ ASSOCIATED CONTENT

Ⓢ Supporting Information

Figures giving 1D and 2D NMR spectra. The Supporting Information is available free of charge on the ACS Publications website at DOI: 10.1021/acs.organomet.5b00370.

■ AUTHOR INFORMATION

Corresponding Author

*L.V.P.: e-mail, luda_parfenova@mail.ru, ink@anrb.ru; tel, +7 347 2843527; fax, +7 347 2842750.

Notes

The authors declare no competing financial interest.

■ ACKNOWLEDGMENTS

The authors thank the Russian Foundation of Basic Research (Grant No. 12-03-33089mol_a_ved), Russian Ministry of Education and Science (Grant No. 8426) and Russian Science Foundation (Grant No. 15-13-00053) for financial support.

■ REFERENCES

(1) (a) Dzhemilev, U. M.; Ibragimov, A. G. *Russ. Chem. Rev.* **2000**, *69*, 121–135. (b) Guiry, P. J.; Coyne, A. G.; Carroll, A.-M. In *Comprehensive Organometallic Chemistry III*; Mingos, D. M. P., Crabtree, R. H., Eds.; Elsevier: Amsterdam, 2007; Vol. *10*, pp 839–869. (c) Dzhemilev, U. M.; Ibragimov, A. G. In *Modern Reduction Methods*; Andresson, P. G., Munslou, J. J., Eds.; Wiley-VCH: Weinheim, Germany, 2008; pp 447–489. (d) Tolstikov, G. A.; Dzhemilev, U. M.; Tolstikov, A. G *Aluminiyorganicheskie soedineniya v organicheskom sinteze (Organoaluminum compounds in organic synthesis)*; Akad. izd. GEO: Novosibirsk, Russia, 2009 (in Russian). (e) Zaidlewicz, M.; Wolan, A.; Budny, M. In *Comprehensive Organic Synthesis*, 2nd ed.; Knöchel, P., Molander, G. A., Eds.; Elsevier Science & Technology: Amsterdam, 2014; Vol. *8*, pp 877–963.

(2) (a) Sato, F.; Sato, S.; Kodama, H.; Sato, M. *J. Organomet. Chem.* **1977**, *142*, 71–79. (b) Ashby, E. C.; Noding, S. A. *J. Org. Chem.* **1979**, *44*, 4364–4371. (c) Ashby, E. C.; Noding, S. A. *J. Org. Chem.* **1980**, *45*, 1035–1041.

(3) Parfenova, L. V.; Khalilov, L. M.; Dzhemilev, U. M. *Russ. Chem. Rev.* **2012**, *81*, 524–548.

(4) Parfenova, L. V.; Pechatkina, S. V.; Khalilov, L. M.; Dzhemilev, U. M. *Russ. Chem. Bull.* **2005**, *54*, 316–327.

(5) Parfenova, L. V.; Vil'danova, R. F.; Pechatkina, S. V.; Khalilov, L. M.; Dzhemilev, U. M. *J. Organomet. Chem.* **2007**, *692*, 3424–3429.

(6) Pankratyev, E. Yu.; Tyumkina, T. V.; Parfenova, L. V.; Khalilov, L. M.; Khursan, S. L.; Dzhemilev, U. M. *Organometallics* **2009**, *28*, 968–977.

(7) Shoer, L. I.; Gell, K. I.; Schwartz, J. *J. Organomet. Chem.* **1977**, *136*, C19–C22.

(8) Baldwin, S. M.; Bercaw, J. E.; Brintzinger, H. H. *J. Am. Chem. Soc.* **2008**, *130*, 17423–17433.

(9) Pankratyev, E. Yu.; Tyumkina, T. V.; Parfenova, L. V.; Khursan, S. L.; Khalilov, L. M.; Dzhemilev, U. M. *Organometallics* **2011**, *30*, 6078–6089.

(10) (a) Soga, K.; Kaminaka, M. *Makromol. Chem., Rapid Commun.* **1992**, *13*, 221–224. (b) Tsai, W. M.; Chien, J. C. W. *J. Polym. Sci., Part A: Polym. Chem.* **1994**, *32*, 149–158. (c) Chen, Y. X.; Rausch, M. D.; Chien, J. C. W. *J. Polym. Sci., Part A: Polym. Chem.* **1995**, *33*, 2093–2108. (d) Forlini, F.; Fan, Z. Q.; Tritto, I.; Locatelli, P.; Sacchi, M. C. *Macromol. Chem. Phys.* **1997**, *198*, 2397–2408. (e) Kleinschmidt, R.; van der Leek, Y.; Reffke, M.; Fink, G. *J. Mol. Catal. A: Chem.* **1999**, *148*, 29–41. (f) Kim, I.; Zhou, J. M. *J. Appl. Polym. Sci.* **2000**, *75*, 843–855. (g) Resconi, L.; Piemontesi, F.; Nifant'ev, I. E.; Ivchenko, P. V. Metallocene compounds, process for their preparation, and their use in catalysts for the polymerization of olefins. U.S. Patent 6,051,728, April 18, 2000. (h) Bravaya, N. M.; Khrushch, N. E.; Babkina, O. N.; Panin, A. N. *Rossijskij Khimicheskij Zhurnal* **2001**, *45*, 56–68 (in Russian). (i) Seraidaris, T.; Löfgren, B.; Mäkelä-Vaarne, N.; Lehmus, P.; Stehling, U. *Macromol. Chem. Phys.* **2004**, *205*, 1064–1069. (j) Ní Bhriain, N.; Brintzinger, H. H.; Ruchatz, D.; Fink, G. *Macromolecules* **2005**, *38*, 2056–2063. (k) Bravaya, N. M.; Panin, A. N.; Faingol'd, E. E.; Babkina, O. N.; Razavi, A. *J. Polym. Sci., Part A: Polym. Chem.* **2010**, *48*, 2934–2941. (l) Sacco, M.; Nifant'ev, I.; Ivchenko, P.; Bagrov, V.; Focante, F. Metallocene compounds. U.S. Patent 7,803,887 B2, Sep. 28, 2010. (m) Resconi, L.; Nifant'ev, I. E.; Ivchenko P. V.; Bagrov, V.; Focante, F.; Moscardi, G. Metallocene compounds. U.S. Patent US 7,858,717 B2, December 28, 2010. (n) Resconi, L.; Focante, F.; Balboni, D.; Nifant'ev, I. E.; Ivchenko P. V.; Bagrov, V. Metallocene compounds. U.S. Patent US 7,834,205 B2, November 16, 2010.

(o) Nejabat, Gh.-R.; Nekoomanesh, M.; Arabi, H.; Salehi-Mobarakeh, H.; Zohuri, Gh.-H.; Omidvar, M.; Miller, S. A. *Macromol. React. Eng.* **2012**, *6*, 523−529.

(11) Baldwin, S. M.; Bercaw, J. E.; Brintzinger, H. H. *J. Am. Chem. Soc.* **2010**, *132*, 13969−13971.

(12) Baldwin, S. M.; Bercaw, J. E.; Henling, L. M.; Day, M. W.; Brintzinger, H. H. *J. Am. Chem. Soc.* **2011**, *133*, 1805−1813.

(13) (a) Khil'ko, A. V.; Spivak, S. I.; Gubaydullin, I. M.; Parfenova, L. V. *Vestnik Bashkirskogo universiteta (Bulletin of Bashkir University)* **2008**, *13*, 843−846 (in Russian). (b) Gubaydullin, I.; Koledina, K.; Sayfullina, L. *Engineering Journal* **2014**, *18*, 13−24.

(14) (a) Ziegler, K.; Kroll, W.-R.; Larbig, W.; Steudel, O.-W. *Liebigs Ann. Chem.* **1960**, *629*, 53−89. (b) Hoffmann, E. G. *Justus Liebigs Ann. Chem.* **1960**, *629*, 104−121. (c) Mole, T.; Jeffery, E. A. *Organoaluminium Compounds*; Elsevier: New York, 1972. (d) Vestin, R.; Vestin, U.; Kowalewski. *Acta Chem. Scand.* **1985**, *39A*, 767−773.

(15) Pankratyev, E. Yu.; Khursan, S. L.; Tyumkina, T. V.; Khalilov, L. M. *J. Struct. Chem.* **2011**, *52*, 27−34.

(16) Eisch, J. J.; Rhee, S. G. *J. Organomet. Chem.* **1972**, *38*, C25−C28.

(17) Eisch, J. J.; Rhee, S. G. *J. Organomet. Chem.* **1972**, *42*, C73−C76.

(18) (a) Woo, H.-G.; Freeman, W. P.; Tilley, T. D. *Organometallics* **1992**, *11*, 2198−2205. (b) Pool, J. A.; Bradley, Ch. A.; Chirik, P. J. *Organometallics* **2002**, *21*, 1271−1277.

(19) (a) Chirik, P. J.; Day, M. W.; Labinger, J. A.; Bercaw, J. E. *J. Am. Chem. Soc.* **1999**, *121*, 10308−10317. (b) Chirik, P. J.; Bercaw, J. E. *Organometallics* **2005**, *24*, 5407−5423.

(20) Freidlina, R. Kh.; Brainina, E. M.; Nesmeyanov, A. N. *Dokl. Acad. Nauk SSSR* **1969**, *138*, 1369 (in Russian).

(21) Reynolds, L. T.; Wilkinson, G. *J. Inorg. Nucl. Chem.* **1959**, *9*, 86.

(22) Piccolrovazzi, N.; Pino, P.; Consiglio, G.; Sironi, A.; Moret, M. *Organometallics* **1990**, *9*, 3098−3105.

(23) Nifant'ev, I. E.; Ivchenko, P. V. *Organometallics* **1997**, *16*, 713−715.

(24) Rybak, B. L. *Analiz nefti i nefteproduktov (Analysis of Crude Oil and Oil Products)*; Gostoptekhizdat: Moscow, 1962.

DOI: 10.1021/acs.organomet.5b00370